THE POTENTIAL OF REMOTE SENSING FOR ENVIRONMENTAL MONITORING

Zoltan Horvat[1*], Mirjana Horvat[1]

[1] Faculty of Civil Engineering Subotica, Subotica, Serbia
* corresponding author: horvatz@gf.uns.ac.rs

Paper type: Original scientific paper
Received: 2024-05-30
Accepted: 2024-11-23
Published: 2024-12-29

UDK: 502.51(497.113PALIĆ)
DOI: 10.14415/JFCE-907

ABSTRACT:

The presented study is aimed at evaluating the potential of remote sensing in environmental monitoring and management. Further aims of the research include examining the satellite image processing level most suitable for this purpose. Essentially, a study area was selected to implement basic environmental analysis using level A2 data from Sentinel-2 images. Although the attained images provide some insight into the site occurrences, it was concluded that attaining a comprehensive understanding of the environment (e.g. exact numerical values of water quality parameters) requires a more comprehensive analysis. The required level of research then asks for the utilization of level C1 images, as they allow the extraction of empirical curves, providing the possibility of their calibration and further implementation. Finally, extracting that type of information would support the initial goal, providing better support for proper environmental monitoring and management.

KEYWORDS:

Remote sensing, environmental monitoring, spectral response, Lake Palic, Lake Ludas

1 INTRODUCTION

Most important contemporary environmental challenges include climate change, reduction of biodiversity, as well as extensive pollution of water, air and soil. The correlation between these factors is well known. As an example, we can consider the hydrological extremes caused by human actions such as building of dams and reservoirs that are structures designed to deliberately alter the hydrological cycle, consequently affecting sediment transport rates, changes in water quality, and eventually modified biodiversity. Another example is the result of developing coastal tourism, as it leads to the concentration of water supply in these areas. At the same time the increase of annual temperatures causing warmer and drier climate will consequently cause increased irrigation requirements, thus further increasing the concentration of water demand, [1]. The need for integral water monitoring and management is well known to the government agencies and there are continual efforts toward achieving this goal. It is essential to implement such a management approach that will include an extensive analysis of the correlation between various factors. This could help improve decision making and eventually help in achieving water resilience.

An example of such interacting decision and consequences is presented in [2] that found a high correlation between areas of reduced resilience and high drainage, and their vulnerability to droughts. Water resistance is essential for providing resilience in other areas as well, and as such has a great impact in numerous ways. For example, stable and high-water levels are necessary for healthy wetlands that can easily be degraded in case of prolonged droughts, whereas wetlands could also be utilized for flood management. If we consider peatlands, they are essential for providing numerous ecosystem services including the uptake of nutrients from water, carbon storage and biodiversity, thus circling back to water resilience.

To tackle the water challenge, we must provide a sustainable solution to specific issues such as ecosystem protection, protection of wetlands and biodiversity, provide drinking water and sanitation, as well as reducing the value of our water footprint. The European Environmental Agency found that the main contributors to river basin water stresses include agriculture, water supply and tourism, resulting in reduced water resource availability [1]. They found that at some locations a 40% river discharge reduction could be expected in summer, determined for a 3˚C rise study. It quickly becomes evident that sustainable water and environment management depends on the capability to provide sustainable data that is essential for the task ahead. Information on water levels, water and air quality, temperature changes, pollution sources and other data need to be provided systematically. Considering the requirements of such data, both temporal and economical, there was an effort to provide a more sustainable monitoring system by relying on remote sensing. The general principle is that there are sensors that can be utilized for systematic, remote data acquisition and that the data acquired this way and be correlated with the essential information required for good water and environment management. This approach would reduce the human factor in the data gathering and processing tasks, consequently making it more sustainable and economically more desirable.

The introduction of remote sensing into environmental monitoring allowed the researchers to carry out various types of studies relying on satellite data for remote areas where systematic field measurements would otherwise be impossible. This type of monitoring provides datasets that are temporally and spatially systematic and can aid in the monitoring of regeneration or deterioration of the selected environmental parameters. Although there are couple of limitations these data sets have, such as cloud coverage, atmospheric issues, limited resolution of freely available datasets, effect of seasonality [3], this approach still provide countless possibilities that introduced significant advances in environmental monitoring.

There are published studies that proved it is possible to employ remote sensing techniques to extract certain water quality parameters [4]. Estimating Chlorophyll-a using satellite data can be considered a well-established procedure for open ocean waters, but is still in a developing stage for optically diverse waters [5]. Although the spectrum of parameters that can be attained this way is currently limited, it still allows the tracking of some data such as chlorophyll-a concentration, turbidity, total suspended solid concentration; coloured dissolved organic matter, total dissolved solids and others. Using hyperspectral remote sensing even allows the users to estimate the values of total phosphorus and total nitrogen [6].

Other potential applications can be found in marine environmental monitoring where remote sensing can be used for early warning, climate change monitoring, biochemical and ecosystem features, marine physical features, marine pollution, and marine aerosols monitoring [7]. A study published by [8] shows one specific usage of remote sensing for marine pollution monitoring such focused on oil spill identification, or contamination by plastic waste. A group of authors [9] developed a new method to detect floating plastic objects in coastal areas relying on hyperspectral data and machine learning algorithms, finding that this approach can be quite effective in the detection of plastic in water. Further potential development in this direction could include additional expansion of remote sensing to micro plastic monitoring.

The importance of considering the environment as an integral system rather than a set of separate elements is essential as these elements (weather, water, soil, air, etc.) all interact and affect each other. Soil characteristics will directly influence the production potential of the given soil. That means that it is just as important to know the presence of pollution in the soil, nutrient elements, as it is to know the water content. Furthermore, proper soil usage in agricultural development is essential to provide sustainable development of any area. Due to human activity, soil degradation became a global issue as it has significant impact on the food scarcity and ecological environments [10]. Hence, employing remote sensing for the evaluation of soil degradation through the monitoring of soil erosion, salinization, desertification, and contamination is crucial. Further possibilities for the application of remote sensing include vegetation classification and differentiation regarding the health status based on remote sensing techniques [11], vegetation classification, etc. Another approach to evaluate soil contamination is through the monitoring of vegetative stress, as presented in [12], which has a high potential in aiding the decision making processes in agriculture.

There have been studies that focused on employing remote sensing for the blue carbon storage changes in salt marshes [13]. Salt marshes are areas including coastal wetlands that are flooded and drained by salt water brought in by the tides. This can be expanded by the well-known fact that providing specific vegetation into lakes with high nutrient content can help reduce the nutrient concentrations. By removing this vegetation (cutting it off and disposing of it) will result in removing the nutrient themselves [14].

By relying on the fact that the electronic processes caused by transitional elements in some minerals lead to reduced absorption features in some wavelengths, and specific characteristics of minerals with OH and CO3 acid groups in others, one can conduct lithological and mineralogical mapping, [15]. Employing remote sensing for the monitoring of environmental parameters such as vegetation status, soil moisture content, water quality and quantity assessment, and flood risk assessment is a fast-developing methodology due to the possibility to cover large and hard to reach areas. Relying on satellite images one can provide monitoring of spatial and temporal resilience changes that can aid better decision making processes for the future.

The presented paper is focused on researching the potential and initial steps for employing remote sensing for the evaluation of the environment.

2 BACKGROUND AND METHODS

As stated previously, the aim of the research is to gain introductory knowledge of the potential and specific steps for utilizing remote sensing for environmental monitoring. To do so, the Authors opted for one satellite data provider, Copernicus. Within the Copernicus programme, we chose a satellite (Sentinel-2) and a level of processing (2A) thus defining the starting point of the research.

2.1 COPERNICUS PROGRAM

The Copernicus programme was initiated as an Earth observation programme that will cover a wide range of applications including climate change, land and cost monitoring, temperature and wildfire, agriculture security, air-pollution, disaster monitoring, and other aspects of the environment. This is provided through satellite missions including Sentinel-1, Sentinel-2, Sentinel-3 and Sentinel-5P. The listed missions all have their own specific target goals. For instance, the main objective of the Sentinel-1 mission is providing data for global mass monitoring, sea-ice monitoring, land-ice monitoring, ocean and marine, maritime and emergency response. Sentinel-2 mission is aimed at providing datasets for the monitoring of land, maritime, security and emergency management, and geophysical measurements. The Sentinel-3 mission is more focused on providing data for ocean and land observation services, hence measuring sea surface topography, sea and land surface temperature, and ocean and land surface colour in order to support ocean forecasting, environmental and climate change monitoring. The Sentinel-5P mission is focused on air quality and pollution, monitoring the ozone layer, aviation safety and climate change.

2.2 SENTINEL-2 MISSION

Sentinel-2 mission is comprised of two satellites placed in the same orbit at the altitude of 786 km, phased by 180˚ providing a high resolution, multi-spectral imaging mission. The cycle length for each satellite is 10 days [16].

Sentinel-2 provides images ranging in 13 bands, including 4 bands of 10 m spatial resolution (red, green, blue and a near infrared band), 6 bands with 20 m spatial resolution (4 narrow bands in the visible near infrared resolution, and 2 shortwave infrared), ad 3 bands with 60 m resolution in space (2 shortwave infrared bands and one ultra-blue band). The band numbers, description, spatial sample distances and central wavelengths are listed in Tab. 1.

Table 1: Sentinel-2 band classification [16]

Band number	Description	Spatial sample distance (m)	Central wavelength (nm)
1	Ultra-blue (coastal and aerosol)	60	443
2	Blue	10	490
3	Green	10	560
4	Red	10	665
5	Visible and near Infrared (VNIR)	20	705
6	Visible and near Infrared (VNIR)	20	740
7	Visible and near Infrared (VNIR)	20	783
8	Visible and near Infrared (VNIR)	10	842
8a	Visible and near Infrared (VNIR)	20	865
9	Short Wave Infrared (SWIR)	60	945
10	Short Wave Infrared (SWIR)	60	1 375
11	Short Wave Infrared (SWIR)	20	1 610
12	Short Wave Infrared (SWIR)	20	2 190

2.3 SPECTRAL CHARACTERISTICS

Electromagnetic spectrum includes the full range of electromagnetic radiation that is divided into separate bands and organized by frequency or wavelength. Starting from high to low frequency we can differentiate the radio waves, microwaves, infrared, visible light, ultraviolet, x-rays, and gamma rays, Tab. 2. The electromagnetic spectrum starts from very long-wavelengths that have low frequencies (radio waves) and extends to short-wavelengths with high frequencies (Gamma rays) that have the most electromagnetic (EM) energy. The wavelength is presented in the unit of length (meters), while the frequency is given in number of cycles per second where one cycle per second equals 1 Hz.

Spectral signature is the reflective behavior of an object in the EM spectrum. It is typically represented by a graph with wavelengths unit on the X-axis and reflected radiation on the Y-axis. Spectral signature is a function of the wavelength that is defined as the ratio of the reflected radiation energy and incident radiation energy on the object. This parameter is important in remote sensing as all matter on earth has a specific spectral reflectance value making it possible to classify it with appropriate sensors.

The interaction between an object and the solar energy includes the emission of energy by the Sun. The energy travels to the Earth where part of it is reflected and travels back to the sensor that can register it. The solar energy can generally be transmitted, absorbed, reflected, scattered or emitted. If the energy is transmitted, it will pass through the medium.

Table 2. Electromagnetic spectrum and matching wavelengths [1]

Region	Sub-region	Wavelength
Radio wave		>0,3 m
Microwave		0,3 m-1 mm
Infrared	Far infrared	1 mm-20 μm
	Long-wave infrared	20 μm-5 μm
	Mid-wave infrared	5 μm -3 μm
	Short-wave infrared	3 μm-1,1 μm
	Near infrared	1,1 μm-0,78 μm
Visible	Red	789 nm-625 nm
	Orange	625 nm-600 nm
	Yellow	600 nm-577 nm
	Green	577 nm-491 nm
	Blue	491 nm-455 nm
	Violet	455 nm-390 nm
Ultraviolet		390 nm-8,82 nm
X-ray		8,82 nm-6 pm
Gamma ray		<6 pm

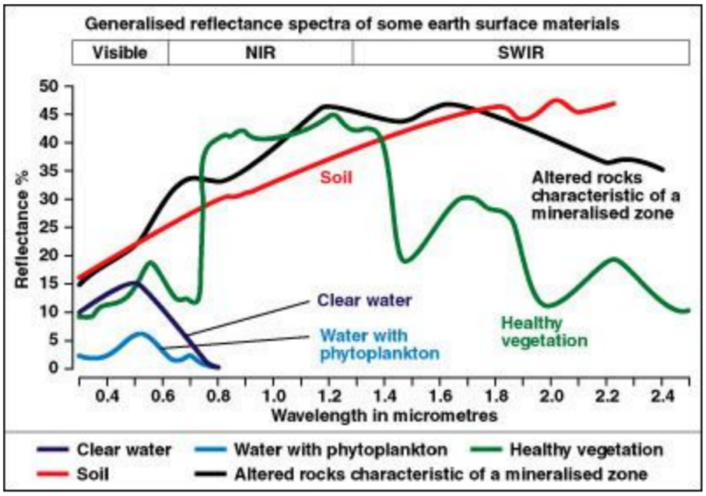

Figure 1: Generalised reflectance spectra of some Earth surface materials, [17]

During this a change of velocity may occur due to refraction because of changing media. If the energy is absorbed, it means it is transferred to the object through the reactions between molecules and electrons. If the energy is reflected, it means it is returned unchanged. Reflectance is the ratio of reflected energy to the incident on a body, where the color of the object is determined by the reflected wavelength. Scattered energy includes random changes in the energy propagation. The emitted energy includes energy that is initially absorbed by the object and afterwards re-emitted by longer wavelengths.

The sensors are allocated to measure the radiance or the brightness in some direction toward the sensor. We defined the spectral signature as the reflection presented as a function of the wavelength. Considering all material have their unique spectral signature, it is used as an identifying tool, Fig. 1.

Figure 1 gives the generalised reflectance values for water, soil, vegetation and some rocks. By carefully inspecting this image we can see that the difference between near infra-red (NIR) reflectance and red reflectance for soil is significantly smaller than the same difference for vegetation. This characteristic is often used for the determination of existence of healthy vegetation through the computation of various vegetation indices Vis, [18].

2.4 DATA ACQUISITION AND PROCESSING

After choosing the data provider, mission and level of processing, one can attend to the acquisition of the satellite images and their processing. The satellite images of Sentinel-2 satellite can be browsed and downloaded from the Copernicus Explore data webpage, [16]. Here one defines the search criteria including satellite, data processing level, cloud coverage, time interval and the area that we need the images for.

In general, the sampled data attained by the sensor is raw and requires various types of data processing techniques. Roughly, the data levels include the following levels: the sampled data level L0 is collected and put through telemetry analysis and preliminary quick look and cloud mask generation to attain L0 consolidated data. Next follow the decompression and SWIR pixels rearrangement to provide L1A data. This data is put through radiometric corrections and geometric viewing and model refinement giving a L1B dataset. After incorporating resampling, conversion to reflectances and preview image and mask generation, we achieve L1C data. Finally, after scene classification and atmospheric correction the L2A data is attained. The image processing levels that are released to the users include level 1C and 2A. Level 1C data is surface reflectance measured at the top of the atmosphere, whereas level 2A data is already processed to provide reflectance at the bottom of atmosphere. The 2A data is ideal for research activities as it allows further analysis without applying additional atmospheric corrections, and can accelerate the research in case the data possibilities are in accordance with the research aim.

The manipulation and evaluation of the satellite images was carried out using the SeNtinel Application Platform (SNAP), that was developed to facilitate the utilisation, viewing and processing of remote sensing data [19].

From Tab. 1 it becomes evident that not all bands have the same resolution. However, to be able to work with the data it is essential to attain uniform pixel size for all band. This is attained through the resampling process where all bands are resampled using the SNAP tool to derive bands with resolution of 10 m.

2.5 AREA OF INTEREST

The Authors chose Lakes Palic and Ludas as the area of interest for this evaluation, Fig. 2. Lake Palic is made up of four sectors labelled as P1 to P4 in the sequence as the water flows through the system. The inflow to P1 is the discharge of treated water from the Wastewater treatment plant in Subotica (WWTPS). The outflow from Palic is through the north-eastern part of P4, where it flows through a small lake into a channel connecting it to Lake Ludas (LN for north and LS for south part of the lake). Issues with water quality within this lake system originate from the structure of the system itself. Namely, the dominant inflow to the system comes from the WWTP, yet there are additional inflows to the system from groundwater, surface runoff, as well as illegal and unsupervised sewage discharge. All these make it extremely difficult to provide exact inflow data, both in terms of quantity and quality, further emphasizing the need for an improved monitoring and management system. All additional information on the selected location and the previously conducted research within this area can be found in [20], [21], [22].

Figure 2: Natural colour representation (B4-B3-B2) of the study area

2.6 BASIC SATELLITE IMAGE ANALYSIS

The study area (Fig. 2) is presented using the natural colour band combinations (B4 red for red, B3 green for green and B2 blue for blue). Even a simple visual inspection of the natural colour image shows distinct differences between the colouring of the first three sectors of Lake Palic, and the fourth sector. Also, there is a notable difference in colour in the north part of Lake Ludas and South part of the Lake. These notable variations in external appearance were the reason to examine these locations, and for the introduced segmentation.

The monitoring of various elements in the environment is based on the already noted characteristics of materials having specific spectral signature [6], hence there is a correlation between the content of a certain material and the reflectance spectrum. As an example, by knowing that vegetation is spectrally distinct from other land cover types, including soil, water, urban areas and others (Fig. 1), we can use this characteristic to develop a special combination of bands and better present the healthy vegetation [18].

It should be pointed out that the SNAP tool includes a set of predefined colour combinations making the visualization of standard band combinations more efficient. The predefined band combinations can naturally be complemented with any colour combination through manual input. Some standard band combinations are given in Fig. 3 and Fig. 4.

Fig. 3 shows the false colour infra-red band combination where the VNIR (B8) is shown as red, the red as green, and green as blue. There are other false colour infra-red band combinations frequently used, consequently the analysis of the image depends on the selected band combination in the specific situation. In this colour combination plants reflect VNIR and green light, while absorbing red. They will reflect more VNIR than green (refer to Fig. 1) making the image areas covered in plants appear deep red (as this band is presented in red). Healthier vegetation also appears as dark red. Clear water will look black, while exposed ground and cities look grey or tan. In case the sediment content of a water body is high, it will reflect green light which is presented in blue colour hence making the water on Fig. 3 look blue. At this point the image manipulation helped in determining information about segments of the Lakes containing both vegetation and some form of sediment in higher concentrations.

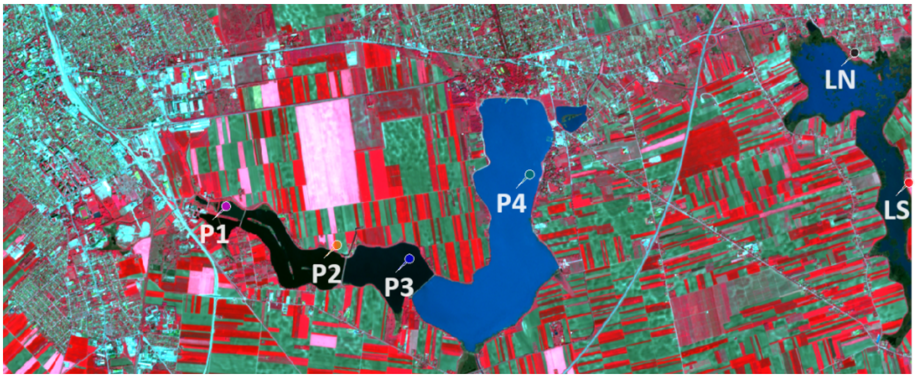

Figure 3: False colour infrared representation (B8-B4-B3) of the study area

Another frequently used band combination in the false colour infra-red view is the B11 for shortwave infra-red in place of the red colour, B8 for the near infra-red in place of green, and B3 green in place of the blue colour, Fig. 4. In this band combination, the water absorbs all three wavelengths, thus it is materialized as black. In case water has notable sediment concentration it will present as blue since sediment particles reflect visible light (in this case green band is reflected, depicted and seen as blue), Fig. 4. Similarly, in case there is saturated soil in the covered area it will also (for this band combination) show up as blue. This is due to the high water content. Namely, as water absorbs all three wavelengths, the object would tend to appear as black, but considering the high particle concentration, that reflect visible light, it will cause this type of water to occur blue. Furthermore, exposed earth will reflect SWIR (displayed as red in the band combination), consequently these areas will come out in red or pink tones. Since plants reflect NIR with high intensity, areas with high vegetation will appear bright green.

Comparison of natural colour and false colour infrared images shows that sector 4 of Lake Palic, and Lake Ludas both have different coloration than the first three sectors of Lake Palic suggesting the presence of chlorophyll, sediment and other optically active matter in the water.

Figure 4: False colour infra-red representation (B11-B8-B3) of the study area

Table 3: Analysis of the sampled pins

Description	Central wavelength	P1 (%)	P2 (%)	P3 (%)	P4 (%)	LN (%)	LS (%)
B1 ultra blue	443	1,90	2,23	2,57	3,89	3,26	2,53
B2 blue	490	2,18	2,35	3,17	4,84	4,46	3,22
B3 green	560	2,11	2,53	3,60	11,36	9,79	6,28
B4 red	665	1,59	1,78	1,99	6,66	5,25	4,02
B5 VNIR	705	1,96	2,11	1,71	10,60	11,62	7,20
B6 VNIR	740	1,72	1,47	1,26	4,45	5,90	3,00
B7 VNIR	783	2,25	1,77	1,37	4,30	5,70	3,03
B8 VNIR	842	2,09	1,60	1,16	3,53	4,72	2,65
B8A VNIR	865	2,04	1,61	1,08	2,68	3,32	1,97
B9 SWIR	945	3,34	1,59	1,16	2,27	1,38	1,21
B11 SWIR	1610	1,94	1,24	0,91	1,27	1,14	1,06
B12 SWIR	2190	1,44	1,08	0,79	1,19	0,97	0,90

Table 3 gives the numerical values of the selected pins. Analysing the presented values band by band can provide us with some valuable information that can easily be verified. Simple analysis shows a notable distinction between reflectance in P1, P2 and P3 and the remaining of the considered water bodies. Further information can be drawn from the previous data by including the findings from a study presented in [23]. The investigation was focused on the reflectance values of Chlorophyll a and b. The results indicated that the concentrations of Chlorophyll a (Chl a) and Chlorophyll a+b can be determined with reasonable precision. Namely, the reflectance near 700 nm is mainly affected by Chl a, while the reflectance at 550 nm is affected by both Chl a, and Chl b. Consequently, total Chl concentration can be determined using both of these wavelengths.

Specific band relations that could be useful are R_{500}/R_{670} that can be managed with the data from Sentinel-2 in bands R_{490}/R_{665} (B2 blue/B4 red), or R_{700}/R_{550}, which is in Sentinel-2 data R_{705}/R_{560} (B5 VNIR/B3 green). The background reflectance can be counteracted by using indices $\frac{R_{700}}{R_{550}} - 1$ or in case of Sentinel-2 $\frac{R_{705}}{R_{560}} - 1$ (B5 VNIR/B3 green-1) or $\frac{R_{670}}{R_{500}} - 1$ that is $\frac{R_{665}}{R_{490}} - 1$ (B4 red/B2 blue -1). The reasoning for the construction of these ratios is that one wavelength is chosen as the sensitive (e.g. B5 VNIR), whereas the other as the insensitive one (e.g. B4 red), since here the absorption processes reach their minimum value, [23].

The physical reasoning for the utilisation of indices is that by combining high reflectance with low reflectance wavelengths, we can enhance selected characteristics on an image. So, by using a simple ratio of near infra-red band divided with the red band, we would attain values near 1 if the monitored area reflects similarly in both areas, while in case of vegetation where the red is mainly absorbed, we would get much higher values (they have high reflectance in NIR and low in R), thus exposing areas with high vegetation presence. As an example, (1) defines a simple ratio for the estimation of vegetation:

$$SR = \frac{R_{705}}{R_{665}} = \frac{B5\ (VNIR)}{B4\ (R)} \tag{1}$$

Using this equation we calculated the following values: $SR_{P1} = 1{,}233$, $SR_{P2} = 1{,}185$, $SR_{P3} = 0{,}859$, $SR_{P4} = 1{,}592$, $SR_{LN} = 2{,}213$, $SR_{LS} = 1{,}791$. What is easily detectable from these values is that there is a notable difference between the values in the first three segments of Lake Palic, and the fourth part of Palic and Lake Ludas. Another value standing out is the SR for the third sector that is less than 1, suggesting the reflectance in red band is greater than in the near infra-red.

An extensive overview of various reflectance indices used for environmental monitoring can be found in [24].

2.7 TEMPORAL ANALYSIS OF SATELLITE IMAGES

The previous analysis introduced some elementary image analysis possibilities, by altering the displayed wavelengths to manipulate the visual data and enhance the visibility of the analysed phenomena. Additionally, one can use various indices to further increase the visibility of the studied surfaces and to tackle issues arising from altered reflectance values due to sun and satellite position. Furthermore, extracting spectral values for chosen points allows us to quantify the observations and conduct more precise analysis.

Another manner in which this data can be evaluated is through temporal inspection, in order to monitor changes occurring over time. To do so, a series of images of the same location were downloaded. The selected timing of the images was such to provide data for the same research area throughout the year. Due to high cloud coverage various dates of satellite images were excluded, resulting in the following dates: June 23rd 2023, August 22nd 2023, September 11th 2023, October 16th 2023, February 3rd 2024, April 13th 2024 and May 13th 2024. The investigated images are given on Figs. 5, 6 and 7. Within every image a point was selected for a more comprehensive analysis. The location of the points is given on Fig. 5. The location of these points was the same for every image in order to obtain a comparable dataset. Comparing the images downloaded at different time intervals one can monitor the annual changes that occur.

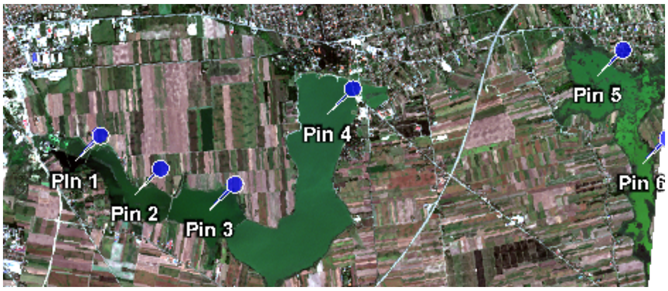

Figure 5: Placement of the selected points within the system

Figure 6: Natural colours June 23rd 2023 (left and August 22nd 2023 (right)

Figure 7: Natural colours September 11th 2023 (left) and October 16th 2023 (right)

Figure 8: Natural colours February 3rd 2024 (left) and April 13th 2024 (right)

By visual inspection of the given images one can easily detect changes occurring through the year in terms of significantly altered water colour. The images are arranged by the acquisition dates, but we should examine them starting from the beginning of the year (Figures 8), as there is a type of reset of vegetation during the winter. On the images from February 3rd and April 13th of 2024 we can notice the water in P1, P2 and P3 is quite clear. Even LS seems relatively clear in winter time, although there are notable changes that occur by April. We can also detect more developed vegetation in April as the green colour is more pronounced suggesting vegetation growth. Images from August and September do not show any significant changes, while by October we can start to observe the reduction in vegetation as the green colour starts to fade away in the sectors closest to the WWTP. One image seems to stand out, the one dating from June 23rd of 2023, where we can see blue-green colouring of P2 and P3. Further analysis requires a more thorough analysis, so a spectral response evaluation has been conducted.

3 RESULTS AND DISCUSSION

To extract a more meticulous understanding of the presented manifestation, the most notable timings have been selected, for which the spectral signatures were determined throughout the considered lake system.

Figures 9, 10 and 11 show the changes of spectral response for the selected timings. Figure 9 is the representation for June 23rd where points indicate the average wavelength. Considering the values given in specific points, the results can only be interpreted in these specific points. A good start for interpretation is at P1, as it clearly follows the expected behaviour. Namely, there is only slight reflectance in the first two bands, and a minor increase in the third (green) that is reflected by vegetation. The next increase is detected at B5 which is a VNIR band and the limit around which vegetation starts to reflect with higher intensity. The highest values are attained at B9 (SWIR), and after that a slow decrease is displayed. Sadly, the reflectance values for B10 are missing, as this is the point around which we would detect the change in tendency of the results.

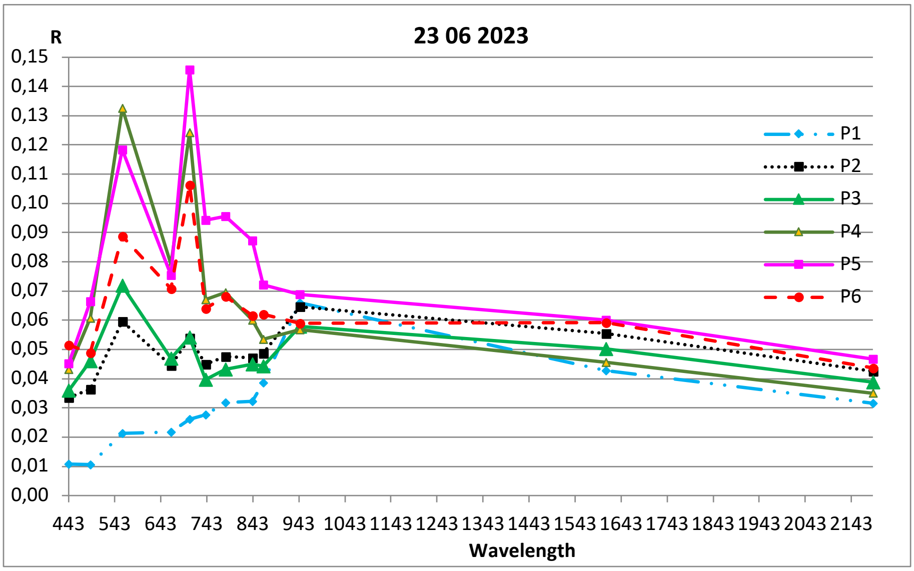

Figure 9: Spectral responses for the selected locations on June 23rd 2023

Another noteworthy occurrence is that there are significant increases of reflectance values for points P4, P5 and P6, although the increase at P6 is noticeably lesser. By comparing the numerical values with the site images, this is an occurrence we would not be able to detect. The attained peaks on the spectral response images coincide with the peaks expected from the typical responses given on Fig. 1.

Figure 10 gives the same values in the summer (August) when the chlorophyll concentrations in the Lakes are still high, which is usually manifested through strong green colour, reduced oxygen values, frequently followed with fish die of.

Figure 11 clearly depicts the reduction of vegetation manifested through the absence of reflectance in B9. The reflectance values are generally very small. The highest values are attained at P4 and P5 in VNIR B5, which is near the limit before the increase of vegetation reflectance. This peak indicates that the described occurrence may be a result of high suspended sediment concentrations.

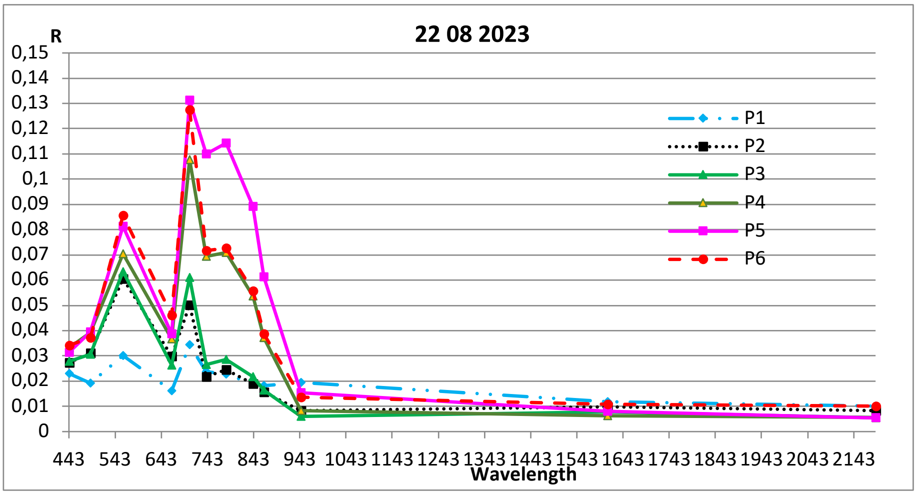

Figure 10: Spectral responses for the selected locations on August 22nd 2023

At this point it is becoming evident that a more in depth analysis would be beneficial to provide a reliable understanding of the presented results. This speculation is supported by the shapes of the graphs presented on Figs. 12, 13, 14 and 15. The Figures show the change of one selected band through the system at the monitored dates.

Consequently, Fig. 12 presents the spatial and temporal change of the reflectance of B4 (green). The influence of vegetation is once again confirmed as there is a notable decrease of reflectance values in the winter time. By closely monitoring the influence of the time of year on the results, one can identify an increasing tendency when moving from winter to the summer.

The previous conclusion can be generalized for all the results, Figs. 13, 14 and 15. Furthermore, we can identify more optical activity in the VNIR region than the visible region (colours green and red). Nevertheless, if comparing red and green reflectance values, there is more activity in the green band, probably due to the presence of vegetation.

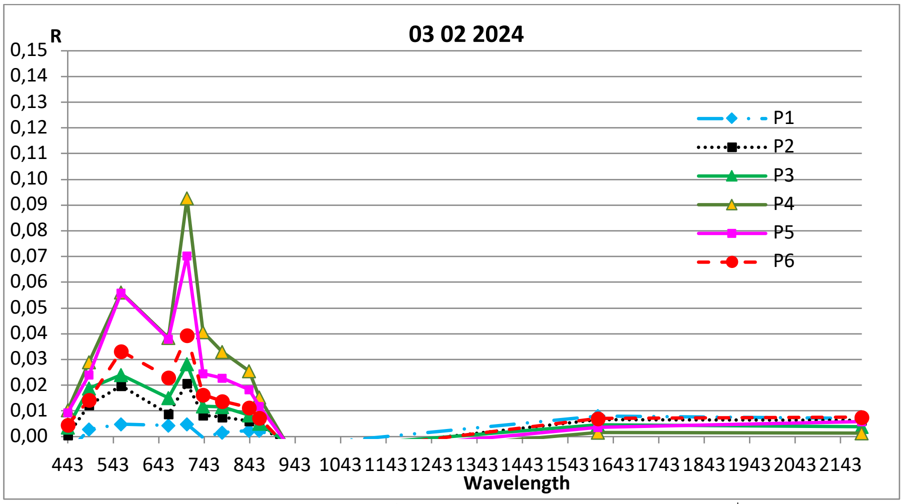

Figure 11: Spectral responses for the selected locations on April 13th 2023

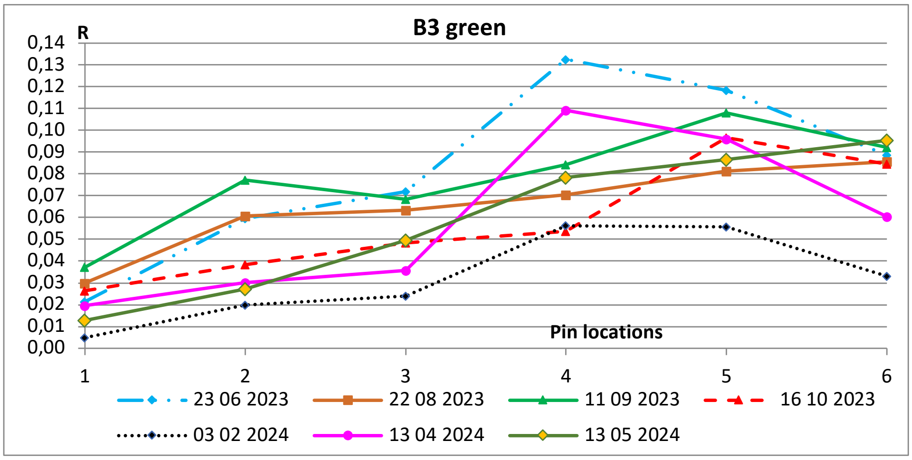

Figure 12: Spectral responses for the selected locations on April 13th 2023

By inspecting results for B11 (SWIR), one can see that there is no notable activity, and this coincides with the tendencies presented on Fig. 1.

The presented overview stands to show that although the application of satellite images has high potential, simply relying on already processed data (L2A) is quite limiting. If LC1 data is downloaded instead of L2A data, it would allow the determination of the pre-processing parameters on one side, but more important, it unlocks the possibility to employ data calibration and the extraction of empirical functions that can be used for the prediction of different water quality parameters.

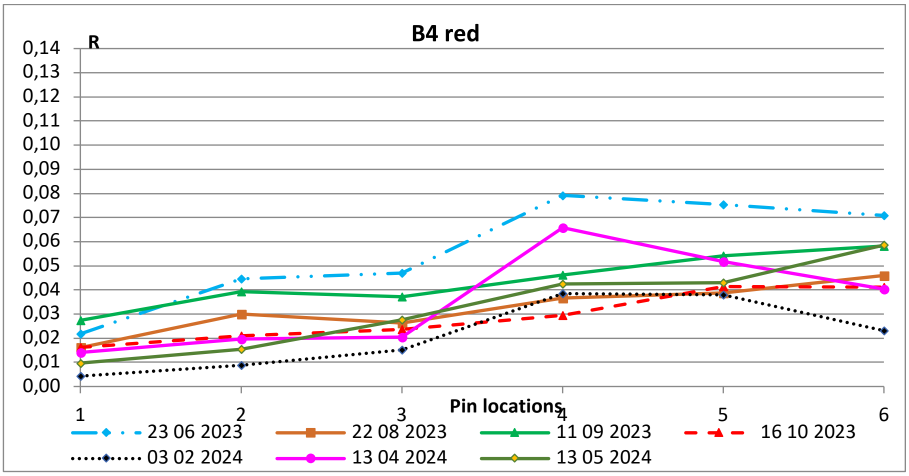

Figure 13: Spectral responses for the selected locations on April 13th 2023

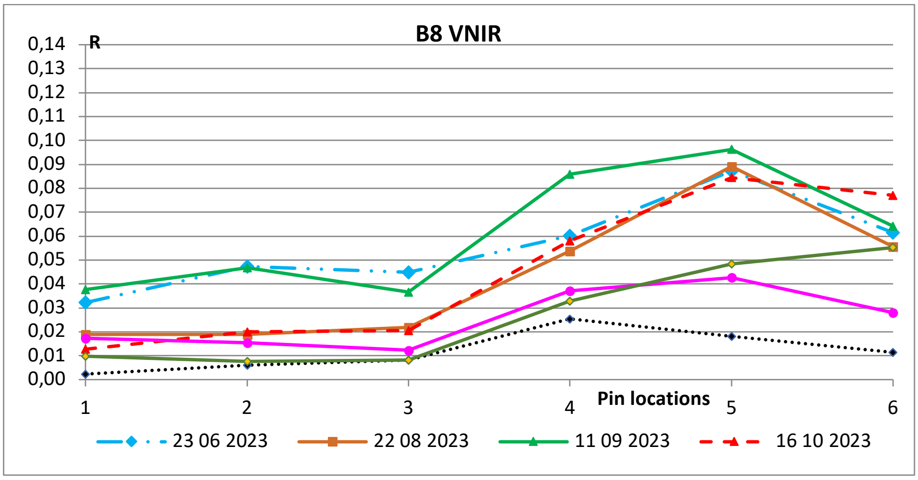

Figure 14: Spectral responses for the selected locations on April 13th 2023

The implication this would have serves the basic goal of this paper, that is, the use of satellite imagery for a more efficient management and monitoring of the water and environment. Top of atmosphere satellite images can be used to extract, e.g., chlorophyll concentrations correlated image parameters. Consequently, by combining that data with in situ measurements, one can obtain a site specific curve providing approximate concentration values depending on the image parameter. Finally, the number of in situ samplings can be reduced (alternately the number of available data can be increased) because of the more frequent availability of satellite images (hence computed concentrations).

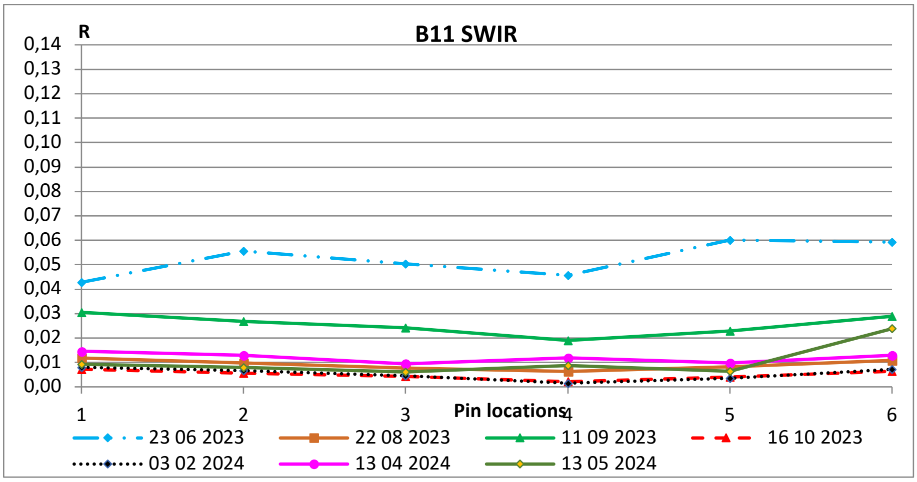

Figure 15: Spectral responses for the selected locations on April 13th 2023

4 CONCLUSIONS

The presented work provides an insight into the potential of employing remote sensing for the monitoring and management of the environment. Furthermore, the paper provides simple guidelines for implementing basic satellite image analysis and estimates its potential use. The idea was to employ Sentinel-2 data of L2A processing as this level of processing allows the fastest way for data retrieval.

The implemented evaluation indicated that although the extracted values of the reflections provide some additional insight, and employing false colour representation can aid the process of distinguishing between regions. However, a more comprehensive understanding of the images requires the utilization of LC1 data. The cause behind this is that it allows the user to employ additional processing techniques that enables the extraction of empirical correlations which can be calibrated using field measurements and can lead to significant improvement in specific data availability. On the other hand, increased data availability is the basic requirement for improved environmental monitoring. Another important implication of such models would be the reduction of human involvement as it is often the limiting factor.

REFERENCES

[1] E. A. European, "Water resources across Europe — confronting water stress: an updated assessment," Publications Office of the European Union, Luxembourg, 2021.

[2] K. J. Lees, R. Artz, D. Chandler, T. Aspinall, C. Boulton, J. Buxton, N. Cowie and T. Lenton, "Using remote sensing to assess peatland resilience by estimating soil surface moisture and drought recovery," *Science of The Total Environment,* vol. 761, 2021.

[3] K. Y. Muhammad Kamran, "Evolution and use of remote sensing in ecological vulnerability assessment: A review," *Ecological Indicators,* vol. 148, 2023.

[4] G. Adjovu, H. Stephen, D. James and S. Ahmad, "Overview of the Application of Remote Sensing in Effective Monitoring of Water Quality Parameters," *Remote Sensing,* vol. 15, no. 7, 2023.

[5] M. Tran, V. Vantrepotte, H. Loisel, E. Oliveira, K. Tran, D. Jorge, X. Mériaux and R. Paranhos, "Band Ratios Combination for Estimating Chlorophyll-a from Sentinel-2 and Sentinel-3 in Coastal Waters," *Remote Sensing,* vol. 15, 2023.

[6] Q. Y. G. &. Q. Z. Cao, "Application and recent progress of inland water monitoring using remote sensing techniques," *Environmental Monitoring and Assessment,* vol. 195, no. 125, 2023.

[7] Y. Shuyun, L. Ying, B. Fangwen, X. Haoxiang, Y. Yuping, Y. Qiushi, Z. Shuqiao, Y. Haoyang, X. Jiajun, H. Ziwei and L. Jian, "Marine environmental monitoring with unmanned vehicle platforms: Present applications and future prospects," *Science of The Total Environment,* vol. 858, no. 1, 2023.

[8] Z. Lin, "Application of Remote Sensing Technology in Chinese Marine Pollution Monitoring," *Highlights in Science, Engineering and Technology,* vol. 83, 2024.

[9] N. Taggio, A. Aiello, G. Ceriola, M. Kremezi, V. Kristollari, P. Kolokoussis, V. Karathanassi and E. A. Barbone, "A Combination of Machine Learning Algorithms for Marine Plastic Litter Detection Exploiting Hyperspectral PRISMA Data," *Remote Sensing,* vol. 14, no. 15, 2022.

[10] J. Z. W. H. S. C. I. L. M. Z. X. Y. Jingzhe Wang, "Remote sensing of soil degradation: Progress and perspective," *International Soil and Water Conservation Research,* vol. 11, no. 3, 2023.

[11] S. I. Elmahdy, M. Marghany and J. Luo, Remote Sensing for Environmental Monitoring, Frontiers Media SA, 2024.

[12] J. R. Dean, S. Ahmed, W. Cheung, I. Salaudeen, M. Reynolds, S. L. Bowerbank, C. E. Nicholson and J. J. Perry, "Use of remote sensing to assess vegetative stress as a proxy for soil contamination," *Environmental Science: Processes & Impacts,* vol. 26, pp. 161-176, 2024.

[13] A. Freitas, J. M. D. and C. L. Lopes, "Application of remote sensing methods for monitoring extent, condition and blue carbon storage in salt marshes," *Remote Sensing Applications: Society and Environment,* vol. 35, 2024.

[14] J. Vymazal, "Removal of Nutrients in Various Types of Constructed Wetlands," *The Science of The Total Environment,* vol. 380, pp. 48-65, 2007.

[15] B. Zoheir, M. A. El-Wahed, A. B. Pour and A. Abdelnasser, "Orogenic Gold in Transpression and Transtension Zones: Field and Remote Sensing Studies of the Barramiya–Mueilha Sector, Egypt," *Remote Sensing,* vol. 11, no. 18, 2019.

[16] Copernicus, “Explore data Copernicus,” [Online]. Available: https://dataspace.copernicus.eu/explore-data.

[17] J. O. Connell, *Monitoring Changes to Irish Peatlands using Satellite Remote Sensing,* Dublin: UCD School of Biosystems Engineering,College of Engineering & Architecture,University College Dublin, 2012.

[18] P. Lemenkova, “Sentinel-2 for High Resolution Mapping of Slope-Based Vegetation Indices Using Machine Learning by SAGA GIS,” *Transylvanian Review of Systematical and Ecological Research,* vol. 22, no. 3, pp. 17-34, 2020.

[19] “SNAP toolboxes,” [Online]. Available: https://step.esa.int/main/toolboxes/snap/.

[20] M. Horvat, Z. Horvat and K. Pastor, “Multivariate analysis of water quality parameters in Lake Palic, Serbia,” *Environmental Monitoring and Assessment,* vol. 193, no. 7, 2021.

[21] Z. Horvat and M. Horvat, “Faculty of Civil Engineering Subotica,” 2020. [Online]. Available: https://www.gf.uns.ac.rs/~zbornik/doc/ZR37.06.pdf.

[22] Z. Horvat and M. Horvat, “Faculty of Civil Engineering Subotica,” 2021. [Online]. Available: https://www.gf.uns.ac.rs/~zbornik/doc/NS2021.45.pdf.

[23] A. A. Merzlyak and M. N. Gitelson, “Signature Analysis of Leaf Reflectance Spectra: Algorithm Development for Remote Sensing of Chlorophyll,” *Journal of Plant Physiology,* vol. 148, pp. 494-500, 1996.

[24] A. Kior, V. Sukhov and E. Sukhova, “Application of Reflectance Indices for Remote Sensing of Plants and Revealing Actions of Stressors,” *Photonics,* vol. 8, no. 12, 2021.

[25] KU Libraries, “How to Select and Use Citation Management Tools: Citation tools in Microsoft Word,” KU Libraries, 22 9 2022. [Online]. Available: https://guides.lib.ku.edu/c.php?g=95057&p=3908473. [Accessed 4 1 2012].

[26] “Copernicus browser,” [Online]. Available: https://browser.dataspace.copernicus.eu/?zoom=5&lat=50.16282&lng=20.78613&themeId=DEFAULT-THEME&visualizationUrl=https%3A%2F%2Fsh.dataspace.copernicus.eu%2Fogc%2Fwms%2Fa91f72b5-f393-4320-bc0f-990129bd9e63&datasetId=S2_L2A_CDAS&demSource3D=%22MAPZEN%22&clo.

[27] Q. Cao, G. Yu and Z. Qiao, “Application and recent progress of inland water monitoring using remote sensing techniques,” *Environmental Monitoring and Assessment,* vol. 195, no. 125, 2023.

[28] J. Wang, J. Zhen, W. Hu, S. Chen, I. Lizaga, M. Zeraatpisheh and X. Yang, “Remote sensing of soil degradation: Progress and perspective,” *International Soil and Water Conservation Research,* vol. 11, no. 3, 2023.

[29] M. Kamran and K. Yamamoto, “Evolution and use of remote sensing in ecological vulnerability assessment: A review,” *Ecological Indicators,* vol. 148, 2023.

[30] S. Sommer, J. Hill and J. Mégier, "The potential of remote sensing for monitoring rural land use changes and their effects on soil conditions," *Agriculture, Ecosystems & Environment,* vol. 67, no. 2-3, pp. 197-209, 1998.